1 **Design and characterization of a semi-open dynamic chamber for measuring biogenic volatile**

2 **organic compounds (BVOCs) emissions from plants**

3 Jianqiang Zeng[1,2,4], Yanli Zhang[1,2,3]*, Huina Zhang[1,2], Wei Song[1,2,3], Zhenfeng Wu[1,2,4], Xinming

4 Wang[1,2,3,4]*

5 [1]State Key Laboratory of Organic Geochemistry and Guangdong Key Laboratory of Environmental

6 Protection and Resources Utilization, Guangzhou Institute of Geochemistry, Chinese Academy of

7 Sciences, Guangzhou 510640, China

8 [2]CAS Center for Excellence in Deep Earth Science, Guangzhou, 510640, China

9 [3]CAS Center for Excellence in Regional Atmospheric Environment, Institute of Urban Environment,

10 Chinese Academy of Sciences, Xiamen 361021, China

11 [4]University of Chinese Academy of Sciences, Beijing 100049, China

12 *Correspondence to*: Yanli Zhang (zhang_yl86@gig.ac.cn) or Xinming Wang (wangxm@gig.ac.cn)

13

Abstract.

With the accumulation of data about biogenic volatile organic compounds (BVOCs) emissions from plants based on branch-scale enclosure measurements worldwide, it is vital to assure that measurements are conducted using well-characterized dynamic chambers with good transfer efficiencies and less disturbance on natural growing microenvironments. In this study, a self-made cylindrical semi-open dynamic chamber with Teflon-coated inner surface was characterized both in the lab with standard BVOC mixtures and in the field with typical broad-leaf and coniferous trees. The lab simulation with a constant flow of standard mixtures and online monitoring of BVOCs by proton transfer reaction-time of flight-mass spectrometry (PTR-ToF-MS) revealed that lower real-time mixing ratios and shorter equilibrium times than theoretically predicted due to wall loss in the chamber, and larger flow rates (shorter residence times) can reduce the adbsorptive loss and improve the transfer efficiencies. However, even flow rates were raised to secure residence times less than 1 min, transfer efficiencies were still below 70 % for heavier BVOCs like α-pinene and β-caryophyllene. Relative humidity (RH) impacted the absorptive loss of BVOCs less significantly when compared to flow rates, with compound specific patterns related to the influence of RH on their adsorption behavior. When the chamber was applied in the field to a branch of a *mangifera indica* tree, the enclosure-ambient temperature differences decreased from 4.5±0.3 to 1.0±0.2 °C and the RH differences decreased from 9.8±0.5% to 1.2±0.1 % as flow rates increased from 3 L min^{-1} (residence time ~4.5 min) to 15 L min^{-1} (residence time ~0.9 min). At a medium flow rate of 9 L min^{-1} (residence time ~1.5 min), field tests with the dynamic chamber for *Mangifera indica* and *Pinus massoniana* branches revealed enclosure temperature increase within +2 °C and CO_2 depletion within -50 ppm when compared to their ambient counterparts. The results suggested that substantially higher air circulating rates would benefit reducing equilibrium time, adsorptive loss and the ambient-enclosure temperature/RH differences. However, even under higher air circulating rates and with inert Teflon-coated inner surfaces, the transfer efficiencies for monoterpene and sesquiterpene species are not so satisfactory, implying that emission factors for these species might be underestimated if they are obtained by dynamic chambers without certified transfer efficiencies, and that further efforts are needed for field measurements to improve accuracies and narrow the uncertainties of the emission factors.

44   **Key words:** Biogenic volatile organic compounds (BVOCs); Semi-open dynamic chamber;

45   Transfer efficiency; Wall loss; Emission rates; Ambient-enclosure differences.

46

Highlights

- A dynamic chamber for measuring branch-scale BVOC emissions is characterized.

- Higher circulating air flow rate increases transfer efficiency and decreases equilibrium time.

- Higher circulating air flow rates reduce enclosure-ambient environmental differences.

- Transfer efficiencies of monoterpene and sesquiterpene species are below 70%.

1 Introduction

Plants can emit a wide range of low molecular volatile organic compounds (VOCs), including isoprene, monoterpenes (MTs), sesquiterpenes (SQTs), oxygenated VOCs (OVOCs, e.g. methanol, acetone) and other reactive VOCs (Guenther et al., 2012). These compounds can be signal molecules for communication within plants, between plants, and between plants and insects (Laothawornkitkul et al., 2009; Šimpraga et al., 2016; Douma et al., 2019), and they are useful tools for plants to protect against biotic (e.g. herbivory) and abiotic (e.g. ozone, drought, heat) stresses (Loreto and Schnitzler, 2010; Holopainen et al., 2017). When emitting into atmosphere, these biogenic volatile organic compounds (BVOCs) can contribute substantially to the formation of ozone and secondary organic aerosol (SOA), and influence the budget of oxidants including hydroxyl radicals (Atkinson and Arey, 2003; de Souza et al., 2018; Di Carlo et al., 2004), and thereby directly and/or indirectly impact air quality and climate on regional and even global scale (Peñuelas et al., 2009; Kleist et al., 2012; Gu et al., 2017; Scott et al., 2017). Due to vital roles played by BVOCs in atmospheric chemistry, their emission inventory has become an indispensable part of air quality and climate models. Global annual emissions of BVOCs are estimated over 1 Pg (10^{15} g) (Guenther et al., 1995), yet these estimations may have large uncertainties (Simpson et al., 1999; Guenther et al., 2006; Zhang et al., 2020) and inaccurate emission factors are among the most important contributors to the uncertainties either regionally or globally (Wang et al., 2011; Guenther et al., 2012; Situ et al., 2014). Therefore, well-designed field works are essential and urgently needed to narrow the uncertainty (Niinemets et al., 2011).

Emissions of BVOCs from plants can be measured on leaf-, branch-, and canopy-scale. Although flux measurements above canopies by relaxed eddy accumulation or eddy covariance can obtain ecosystem-scale emission fluxes (Spirig et al., 2005; Rinne et al., 2007; Bai et al., 2017), enclosures on leaf and branch scales are the most convenient and widely-used approaches to measure BVOCs emission from plants (Chen et al., 2019; Huang et al., 2020). These enclosures can be static and dynamic. Static enclosure isolates leaves or branches from the ambient completely, and environmental parameters (e.g. temperature, relative humidity (RH), CO_2 concentration) in the enclosure may deviate far from the ambient. Temperature in the enclosure is likely to increase due to greenhouse effects, humidity increases because of leaf transpiration and CO_2 concentration depletes as a result of photosynthetic consumption by leaves (Kesselmeier et al., 1996; Aydin et al.,

5

83 2014). These will change the physiological state of plants and cause abnormal emissions (Ortega

84 and Helmig, 2008). For this reason, static or semi-static enclosures are considered to be screening

85 tools to verify emitters and non-emitters (Niinemets et al., 2011; Li et al., 2019). Unlike static

86 enclosure, dynamic enclosure introduces circulating air and can reduce the differences in

87 environmental parameters between the enclosure and the ambient to a great extent. Therefore,

88 dynamic enclosure is more reliable and preferred for measuring emissions of BVOCs from plants

89 (Ortega and Helmig, 2008; Pape et al., 2009; Kolari et al., 2012). However, large differences still

90 exist for dynamic enclosure if air exchange is slow. For example, temperature deviation of more

91 than 10 °C between enclosure and the ambient was observed when using dynamic enclosure for

92 field studies (Aydin et al., 2014). This way the measured emission reflects that under a temperature-

93 disturbed environment and therefore might not well represent the real situations. In addition to

94 deviations of environmental parameters in enclosures, adsorption of terpenes can occur on most

95 parts of the enclosure system, including chamber walls, gasket surfaces, and system tubing

96 (Niinemets et al., 2011). The materials used to construct enclosures, like neoprene and low-density

97 polyethylene polymers, are thought to have potentially significant adsorption of VOCs (Niinemets

98 et al., 2011 for a review), resulting in underestimation of emission rates.

99 An ideal dynamic enclosure for measuring emissions of BVOCs from plants should be one without

100 changing the physiological state of the enclosed plant parts, and without introducing pollutions or

101 causing systematic losses. Ortega et al. (2008) used ice water bath and copper tube to drop the

102 temperature and humidity of the circulating air, thereby reducing the deviations of enclosure

103 environmental parameters from the ambient. Aydin et al. (2014) also used circulating cooling water

104 to reduce the temperature of the circulating air, but the temperature inside the enclosure is still much

105 higher than that of the ambient. Kolari et al. (2012) evaluated the performances of dynamic chamber

106 in uncontrolled field environment, the results indicate that the systematic losses of VOCs are higher

107 in wet environment or under high relative humidityRH. Lüpke et al. (2017) tested the chamber wall

108 effects of an environmentally controlled dynamic chamber using Δ^2-Carene in the laboratory. Their

109 results demonstrated that there were no chamber wall effects for Δ^2-Carene but there did exist

110 background contaminations for some other compounds. To date, although there are a variety of

111 dynamic chambers, including sophisticated enclosures designed for laboratory measurements

112 (Copolovici and Niinemets, 2010; Lüpke et al., 2017; Mozaffar et al., 2017) and simple and user-

friendly enclosures for field measurements (Matsunaga et al., 2011; Helmig et al., 2013; ~~Wiß~~Wiss et al., 2017), the performances and wall effects of most dynamic enclosures, particularly those used in the field, are not systematically characterized, and this would lead to difficulties in comparing results from various field measurements. Therefore, in order to pool together the measurement results worldwide to generate a quality dataset that can be shared by the scientific community, it is imperative to get the dynamic enclosures systematically characterized before they are used in the field to measure emissions of BVOCs.

This paper describes a semi-open dynamic chamber for measuring BVOCs emissions from plants. The purpose of this work is to present a protocol demonstrating how the performance of a dynamic chamber can be characterized and optimized for measuring branch-scale emissions of BVOCs. To obtain more accurate BVOC emission rates from plants grown in the field, some most important aspects, including enclosure-ambient differences in environmental parameters (light, temperature and ~~relative humidity~~RH), equilibrium time and wall effects, are assessed and discussed in this study.

2 Descriptions of the semi-open dynamic chamber system

2.1 Design of the semi-open dynamic chamber system

The semi-open dynamic chamber is a cylindrical structure (Fig. 1) made of polymethyl methacrylate, and its inner surface is coated with fluorinated ethylene propylene (FEP) Teflon film (FEP 100, Type 200A; DuPont, USA). It has a volume of 13.7 L with a diameter of 250 mm and a height of 280 mm. Ambient air is drawn into the enclosure with a pump at a constant flow through the front panel whose inner-chamber side is coated with Teflon film (air inlet). A~~n~~ customized PTFE electric Teflon fan (Shenzhen Shuangmu Plastic Material Co. Ltd, China) that driven by an electric motor (BLDC4260, Shenzhen Mingyang Motor Co. Ltd, China) is secured in the middle of inner side of the inlet panel to establish homogeneous chamber conditions; and small holes (5 mm I.D.) are drilled at the edge and ambient air entering from the small holes can flush the inner wall of the chamber and thus reduce the possible occurrence of water condensation on the inner wall. The outlet is covered by polymethyl methacrylate panel which is also coated with FEP Teflon film at the inner-chamber side and joined to the main chamber body by screw. Four holes (Fig. 1) are drilled on the panel: the hole (10 mm I.D.) in the middle is used to seal the branch around the trunk side; the hole "1" (10 mm I.D.) is used to connect temperature and ~~relative humidity~~RH sensor (~~HP32~~HC2A-S,

带格式的: 段落间距段前: 0.5 行, 段后: 0.5 行

7

Rotronic, Switzerland); the hole "2" (10 mm I.D.) is used to connect to adsorption cartridges for sampling BOVOCs for offline analysis; and "3" (10 mm I.D.) is used to connect to the air pump and online analyzers. In order to avoid artificial disturbance to branches when installing the chamber, the polymethyl methacrylate board is cut into two pieces (Fig. 1), which are spliced together after branches are enclosed in the chamber. The gaps between the hole and the trunk are sealed by FEP Teflon tapes. All the tube lines (1/8" inch O.D.) used in the system are PTFE-made while the Swagelok tube fittings are PFA-madeing lines in the system are Teflon made. The An air pump (MPU2134-N920-2.08, KNF, Germany) is equipped with a flowmeter and a mass flow controller (Alicat Scientific, Inc., Tucson, AZ, USA) is used to maintain a constant flow rate (F_1) of the main airflow. Concentrations of CO_2 and H_2O inside and outside the chamber are monitored by infrared gas analyzer (Li-7000; Li-Cor Inc., Lincoln, USA). A proton transfer reaction-time of flight-mass spectrometer (PTR-ToF-MS; Ionicon Analytik GmbH, Innsbruck, Austria), which has time resolution up to one second, is used to monitor the real-time concentrations of BVOCs inside the chamber. More detail descriptions about the determination of BVOCs by the PTR-ToF-MS can be found elsewhere (Wang et al., 2014; Huang et al., 2016; Zhang et al., 2020). Airflow for online analyzers was shunted from the main airflow through hole "3".Flow rates of online analyzers (F_2, 200 ml min^{-1} for PTR-ToF-MS and F_3, 500 ml min^{-1} for Li-7000) and automatic sampler (F_4, 200 ml min^{-1}) are controlled by their built-in MFCs, and total flow rate ($F = F_1 + F_2 + F_3 + F_4$) of circulating air is the sum of these flows and is used to calculate emission rates. In addition, the accurate flow rate ($F_1 + F_2 + F_3$) through hole "3" is measured by a soap-membrane flowmeter (Gilian Gilibrator-2, Sensidyne, USA) before and after each measurement in the field. Temperature and relative humidity (RH) are measured by sensors (HC2A-S, Rotronic, Switzerland), one is installed inside of the chamber and the other is installed outside. Four thermocouples (HTK305000, OMEGA, USA) are used to monitor air temperature inside the chamber and another two thermocouples (ST-50, RKC, Japan) are used to monitor leaf temperature. And temperature and humidity data are recorded by a data logger (HR7000, Zhejiang Jiangheng Instrument equipment Co. Ltd, China). A light sensor (Li-1500; Li-Cor Inc., Lincoln, USA) is installed on the top of the chamber to monitor the photosynthetically active radiation (PAR). After each measurement, branches in the enclosure are harvested and brought back to the lab to determine the dry mass of leaves with a heat oven at 60 °C for 48 hours.

2.2 Collection of offline BVOCs samples and lab analysis

Apart from online measurement by PTR-ToF-MS, offline BVOC samples are also collected since PTR-ToF-MS cannot differentiate isomers of MTs and SQTs. The air is drawn through an ozone scrubber followed by solid adsorbent cartridges (Tenax TA/Carbograph 5TD, Marks International Ltd, UK) using an automatic sampler (JEC921, Jectec Science and Technology, Co., Ltd, Beijing, China) at a flow rate of 200 mL min^{-1} for 10 minutes (Fig. 1). ~~Ambient air s~~Samples of inlet air are collected concurrently in the same way with another automatic sampler to determine the background concentration (C_0) (Fig.1). The collected samples are stored in a portable refrigerator at 4 °C in the field and at -20 °C after brought back to the lab. In the lab, these samples are analyzed by an automatic thermal desorption system (TD-100, Markes International Ltd, UK) coupled to a model 7890 gas chromatography (GC) with a mode 5975 mass selective detector (MSD) (Agilent Technologies, Inc., California, USA). The adsorbent cartridges are thermally desorbed by the TD-100 at 280 °C for 10 minutes and then the desorbed analytes are transferred by pure helium into a cryogenic trap (U-T11PGC-2S, Markes International Ltd, UK) at -10 °C. Then the trap is rapidly heated to transfer the analytes to the GC/MSD system with a capillary column (Agilent, HP-5MS, 30 m × 0.25 mm × 0.25 μm). The GC oven temperature is programmed to be initially at 35 °C (held for 3 minutes), then increase to 100 °C at 5 °C min^{-1} and hold for 3 minutes, to 150 °C at 10 °C min^{-1} and hold for 3 minutes, and then to 280 °C with a final hold time of 2.5 minutes. The MSD is operated in selected ion monitoring (SIM) mode, and the ionization method is electron impacting. The calibration standards were prepared by dissolving the pure liquid standards (Table S1) into n-hexane solution (Kajos et al., 2013; Fang et al., 2021) and ~~-~~diluted to six concentration levels. 1 μL of each standard solution with specific concentration was injected into an adsorbent cartridge and swept with pure helium at 100 mL min^{-1} for two minutes to scavenge n-hexane, and then run the same way as real samples by the TD-GC/MSD system. The chromatogram of standards was showed in Fig S1. Six-point calibration curves (Fig S2; S3) were used to quantify the compounds of interest. Method detection limits (MDLs) were determined by seven parallel analysis of the lowest concentration of calibration standards. The ~~method detection limits (~~MDLs~~)~~ varied from 5 to 17 ng m^{-3} for MTs and from 1 to 8 ng m^{-3} for SQTs. The MDL for isoprene was 56 ng m^{-3} (Table S1).

2.3 Ozone scavenging

Ozone (O$_3$) may impact emissions of BVOCs from plants (Feng et al., 2019). While many dynamic

9

202   enclosures use purified air as circulating air (Chen et al., 2020; Jing et al., 2020), the semi-open

203   dynamic chamber, using ambient air as circulating air in order to reflect BVOCs emission from

204   plants in real atmosphere, need to take the effect of ozone into consideration. On the other hand, the

205   highly reactive BVOCs in atmosphere can be oxidized by oxidants like ozone, especially for MTs

206   and SQTs (Atkinson and Arey, 2003). For our semi-open dynamic chamber with volume of 13.7 L,

207   when the flow rate is set to be 9-12 L min^{-1}, the residence time of circulating air will be within 1.5

208   minutes, far below the lifetimes of some important BVOCs in the atmosphere, which are varying

209   from tens of minutes to tens of hours when reacting with ozone (Atkinson and Arey, 2003).

210   Therefore, losses of BVOCs due to reaction with ozone in the chamber can be ignored according to

211   some previous studies (Kolari et al., 2012; Bourtsoukidis et al., 2012; Helin et al., 2020). However,

212   for the sorbent cartridges used to take BVOCs samples for off-line analysis (Chen et al., 2019; Aydin

213   et al., 2014), ozone will be adsorbed together with BVOCs, resulting in losses of BVOCs due to

214   reaction with ozone in the cartridges during the deliver and storage of the cartridges before lab

215   analysis (Pollmann et al., 2005; Ortega and Helmig, 2008).

216   Potassium iodide (KI) and sodium thiosulfate (Na$_2$S$_2$O$_3$) are widely used for ozone removal during

217   sampling BVOCs with adsorbent tubes (Helmig et al., 2006; Helmig et al., 2007; Aydin et al., 2014;

218   Yaman et al., 2015; Chen et al., 2020). In this study, four types of ozone scrubbers including KI

219   filter, Na$_2$S$_2$O$_3$ filter, KI tube and Na$_2$S$_2$O$_3$ tube were prepared. The KI/Na$_2$S$_2$O$_3$ filters were prepared

220   by cutting quartz fibre filter (23.4×17.6 cm^2; Whatman) into circles, getting them soaked in saturated

221   KI or Na$_2$S$_2$O$_3$ solution and then dried in at 50 °C. The KI/Na$_2$S$_2$O$_3$ tube filters were prepared with

222   copper tubes (1/4" inch in I.D. × 50 cm length) by injecting 5 mL saturated KI/Na$_2$S$_2$O$_3$ solution

223   and then swept to dry with nitrogen. As showed in Fig. S1S4, air flow with ozone concentration of

224   about 100 ppb, which is the daytime peak level that can occur in our study area (the Pearl River

225   Delta region), was generated by an ozone generator and passed through the ozone scrubbers. Ozone

226   analyzer (EC9810, Ecotech, Australia) was used to monitor ozone concentration before and after

227   passing through the scrubbers. All of the ozone scrubbers have ~100 % ozone removal efficiency

228   (Table S2), which means that all of them can effectively scavenge ozone. Besides, to test if any

229   losses of BVOCs happened in the scrubbers, a mixture of BVOCs (~ 20 ppb in nitrogen) was passing

230   through the ozone scrubbers at the same flow rate of 200 mL min^{-1} as normal field sampling, and

231   the concentrations of BVOCs were monitored before and after passing through the scrubber using

232 the PTR-ToF-MS (Fig. S2S5). The results revealed that the recoveries of BVOCs on average were

233 10.05 %, 100.89 %, 100.63 % and 66.70 % for KI filter, $Na_2S_2O_3$ filter, KI tube and $Na_2S_2O_3$ tube,

234 respectively (Table S2). Therefore, both $Na_2S_2O_3$ filter and KI tube can be used to scavenge ozone

235 with good recoveries. Here $Na_2S_2O_3$ filters were used to scavenge ozone as in previous studies

236 (Helmig et al.,2006; 2007).

2.4 Optimization of flow rates

238 The air flow rate is the most important parameter that influence the equilibrium time, the transfer

239 efficiency, the enclosure-ambient differences in temperature and RH, and the steady state

240 concentration of BVOCs as well. Firstly, we tested equilibrium time and transfer efficiency using

241 standard mixtures in the laboratory under 25 °C. The standard mixtures contained representative

242 species emitted from plants, including acetonitrile, acrylonitrile, acrolein, acetone, isoprene,

243 methylacrolein, α-pinene and β-caryophyllene (Table S32); they were prepared in pure nitrogen with

244 concentrations of 300-600 ppbv and compressed into a stainless steel canister with a pressure of 40-

245 50 mbar in the same way by Rhoderick and Lin (2013) and Mermet et al. (2019). As shown in Fig.

246 2, this standard gas mixture was released into the chamber at a constant flow rate to simulate the

247 emission of VOCs from enclosed plant branches with a constant emission factor. While the

248 equilibrium time was tested at flow rates of 3, 6, 9, 12 and 15 L min^{-1} (dry air, RH=0 %) in the lab,

249 the transfer efficiency was further tested in the lab with flow rates of 3, 6, 9, 12 and 15 L min^{-1} and

250 under RH of 20 %, 40 %, 60 %, 80 % and 100 %, respectively. The RH of circulating air was

251 adjusted by mixing dry air (RH=0 %) with humidified air (RH=100 %). All the flow rates were

252 controlled by mass flow controllers (MFCs) (Alicat Scientific, Inc., Tucson, AZ, USA) and

253 calibrated by a soap-membrane flowmeter (Gilian Gilibrator-2, Sensidyne, USA). The real-time

254 concentrations of the standard mixtures in the chamber were measured by PTR-ToF-MS, and the

255 concentrations of these VOCs stored in the stainless steel canister were also measured by PTR-ToF-

256 MS before introduced into the chamber. Acetonitrile, acrylonitrile, acrolein, acetone, isoprene,

257 methylacrolein, α-pinene and β-caryophyllene were detected with m/z 42.019, 45.015, 57.073,

258 59.052, 69.060, 71.040, 137.072 and 204.986, respectively. Transfer efficiency for each compound

259 is expressed as the ratio (%) of outgoing air concentration and incoming air concentration at steady

260 state. Mixing ratios of each compound in the standard mixture stored in the stainless steel canister

261 were initially measured by PTR-ToF-MS. The standard mixture was mixed with pure dry air and

11

262 the mixing ratio of each compound (C_1) in this mixed air was measured by PTR-ToF-MS. This

263 mixed air was switched into the camber at a constant flow to simulate BVOCs emissions from

264 enclosed plant branches, and the steady state mixing ratios of each compound (C_2) in the chamber

265 was again measured by PTR-ToF-MS. Transfer efficiency (%) of each compound was then

266 calculated as the ratio of C_2/C_1. Mixing ratios of acetonitrile, acrylonitrile, acrolein, acetone,

267 isoprene, methylacrolein, α-pinene and β-caryophyllene were determined by PTR-ToF-MS with m/z

268 42.019, 45.015, 57.073, 59.052, 69.060, 71.040, 137.072 and 204.986, respectively.

269

270 **2.5 Field tests**

271 The influence of flow rate on enclosure-ambient differences in temperature and RH was carried out

272 in the campus of Guangzhou Institute of Geochemistry (GIG) with branches of *Mangifera indica* (a

273 broad-leaved isoprene emitter) under sunny and cloudless days with small winds. Totally about 7.0

274 g dry mass of leaves were enclosed in the chamber. The ambient air temperature was 31-33 °C and

275 PAR was 1000-1200 μmol m^{-2} s^{-1}. The enclosure and ambient temperature/relative humidityRH were

276 measured by calibrated sensors (HP32HC2A-S, Rotronic, Switzerland) under circulating air flow

277 rates of 3, 6, 9, 12 and 15 L min^{-1}.

278 Field tests were also carried out during 9:00-17:30 local time (UTC+8) on 8 October 8th 2019 in the

279 Guangdong Tree Garden (23.20° N, 113.38° E) of the Guangdong Academy of Forestry in

280 Guangzhou, south China. The coniferous pine trees are typical monoterpene emitters (Aydin et al.,

281 2014). *Pinus massoniana*, which is a widely distributed pine tree species in south China (Gu et al.,

282 2019; Wang et al., 2019) was selected for our field tests. Healthy nature-grown branches of *Pinus*

283 *massoniana* (~20-year-old and ~12 m high) were enclosed in the dynamic chamber (Fig. 1), and

284 environmental parameters inside and outside of the chamber were compared only under a medium

285 circulating air flow rate of 9 L min^{-1}.

286 **3 Results and discussion**

287 3.1 Equilibrium time

288 Theoretically concentrations of BVOC species that emitted by plant leaves inside a dynamic

289 chamber can be described as below (Niinemets et al., 2011):

290 $$V \frac{dC}{dt} = E - F (C - C_0) \qquad (1)$$

12

where V (L) is the volume of the chamber, E (μg min~~h~~$^{-1}$) is the emission rates of BVOCs~~;~~, C_0 (μg

L^{-1}) ~~is~~ are background concentrations of the BVOC species in air entering into the chamber, which

were determined by PTR-ToF-MS in the lab tests, and in field tests were determined both online by

PTR-ToF-MS and offline by sampling ambient air near the inlet with adsorbent cartridges followed

by TD-GC/MSD analysis back to the lab; ~~and~~ C (μg L^{-1}) is the concentrations of the BVOCs species

in air exiting the chamber~~;~~, and F (L min^{-1}) is air flow rate through the chamber. The above equation

can be expressed explicitly for changing $C(t)$ with time t as below:

$$C(t) = C_0 + \frac{E}{F} \times (1 - e^{-\frac{F}{V} \cdot t}) \qquad (2)$$

Based on the above Eq. (2), with prolonged time t, $C(t)$ will approach a steady state concentration

C_s:

$$C_s = C_0 + \frac{E}{F} \qquad (3)$$

and then E can be calculated as

$$E = F \times (C_s - C_0) \qquad (4)$$

With leaf dry mass (m, g), the emission factors (EF, μg g^{-1} min^{-1}) of enclosed leaves can be

expressed as

$$EF = F \times (C_s - C_0)/m \qquad (5)$$

As showed in Eq. (2), the F/V value, which is the reciprocal of residence time (V/F), determines

how fast a steady state will reach. At a given E, a lower F will result in a longer time to reach steady

state but a higher steady state concentration that benefits instrumental measurements, and vice versa.

In the field measurements, we prefer a shorter equilibrium time to track the variation of emission

rates with changing environment parameters (like PAR) if E/F is well above the method detection

limits. In fact, as showed in Fig. ~~S3~~S6, theoretically steady state concentrations inside the enclosure

would decrease with the increasing flow rates. However, even at flow rates as high as 50 L min^{-1}

(residence time <15 seconds), if leaves with 5.0 g dry mass are enclosed, a BVOC species with an

extremely low emission rate of 0.01 μg g^{-1} h^{-1} would have predicted steady state concentration of

~10 μg m^{-3}, which is still well above the method detection limits (Table S1) of SQTs that typically

have much lower emission rates when compared to isoprene and MTs. Therefore, the influence of

circulating air flow rates on the detection of BVOCs is not an important issue to limit the

performance of the dynamic enclosure method and thus will be not discussed hereafter.

13

3.1 Equilibrium time

Equilibrium time is vital for evaluating the performance of a dynamic chamber. Base on Eq. (2), if $t=3\times V/F$ (3 cycles of residence time), $e^{-(F/V\times t)}\approx0.05$; and if $t=5\times V/F$ (5 cycles of residence time), $e^{-(F/V\times t)}<0.01$, and in this case it can be concluded with confidence that after 5 cycles of residence time the equilibrium or the steady state is reached. With the high time resolution online monitoring by PTR-ToF-MS, equilibrium time could be determined more directly in our lab tests.

Figure 3 shows real-time concentrations of VOCs in the chamber at a flow rate of 9 L min^{-1} when using a standard mixture to imitate the BVOC emission in the lab (Fig. 2). The mixing ratios of VOCs in the chamber increased with time and became stable after ~3-6 minutes or ~2-4 cycles of residence time (Fig. 3). The representative VOC species differs in their times reaching steady state, varying from ~3 minutes for α-pinene to ~6 minutes for acetone and acrylonitrile. The equilibrium time are all within the 5 cycles of residence time (7.5 min).

The real-time mixing ratios of VOCs in the chamber changed in a pattern that was in fairly good agreement with that theoretically predicted by above Eq. (2); however, they were all close and consistently lower than the theoretically predicted values (Fig. 3). The gaps between the measured and predicted values seemed to be larger for heavier BVOC compounds (e.g. α-pinene and β-caryophyllene) than lighter species (e.g. isoprene). Also as showed in Fig. 3, after the stop of injecting the standard mixture, the mixing ratios inside the chamber dropped to their initial background values in a way that was fitted well with theoretical prediction.

The lower than predicted steady-state concentrations were largely due to losses of VOCs in the chamber, which would result in a lower C_s in Eq. (3) and thereby a lower "real" E by Eq. (4). Therefore, apart from equilibrium time, the loss or transfer efficiency must be further considered for an accurate emission measurement by a dynamic chamber.

3.2 Transfer efficiency

Adsorption losses of BVOCs can be a significant fraction in enclosure systems (Helmig et al., 2004). Although Tedlar or Teflon films, which are chemically inert with low surface uptake rates for BVOCs, were used for most dynamic enclosures to diminish the adsorption in the enclosure (Ortega and Helmig, 2008; Gomez et al., 2019; Chen et al., 2020), adsorptive losses cannot be completely eliminated. Kolari et al. (2012) observed 6-29 % compounds losses in a chamber made of transparent acrylic plastic with Teflon-coated inner surfaces. Hohaus et al. (2016) observed average losses of

350   15 % in their enclosure consisting of FEP film. In this study, to assess the adsorptive losses and

351   transfer efficiencies, tests were conducted under different flow rates and RH in the lab with the

352   standard mixture (Fig. 2).

353   **3.2.1 Influence of flow rate on transfer efficiency**

354   Figure 4 shows transfer efficiencies under air circulating rates (dry air) of 3, 6, 9, 12 and 15 L min^{-}

355   ^{1}. Transfer efficiencies of all species increased when flow rates increased from 3 to 15 L min^{-1}, such

356   as from 41.9±2.6 % to 85.4±4.6 % for acetonitrile, 56.5±5.5 % to 90.8±8.7 % for acrylonitrile,

357   24.7±3.0 % to 65.4±2.8 % for acrolein, 42.5±3.5 % to 110.9±2.9 % for acetone, 48.4±4.6 % to

358   106.9±8.3 % for isoprene, 40.6±5.2 % to 92.8±5.8 % for methylacrolein, 26.6±3.2 % to 69.7±3.7 %

359   for α-pinene, and 22.8±3.4 % to 65.9±3.8 % for β-caryophyllene.

360   Transfer efficiencies were apparently unsatisfactory at lower flow rates. For example, at a flow rate

361   of 3 L min^{-1}, for the most important BVOC species like isoprene and α-pinene, their transfer

362   efficiencies on average were as low as 48.4 % and 26.6 %, respectively (Fig. 4). This confirms that

363   larger losses might occur if a static chamber is used to measure emission rates. Even at a flow rate

364   of 15 L min^{-1} (residence time < 1 min), transfer efficiencies were still below 70 % for acrolein, α-

365   pinene, and β-caryophyllene (Fig. 4) although fairly good transfer efficiencies (85 %-111 %) were

366   observed for other species. This result implies that measured emission rates from branches in

367   enclosures might be seriously flawed in case transfer efficiencies are not well characterized and

368   optimized.

369   For a given volume chamber, a higher flow rate is associated with a lower residence time (V/F).

370   More adsorptive losses would occur at longer residence time since VOCs have more time to adsorb

371   onto chamber inner surfaces (Kolari et al., 2012). Therefore, the VOCs loss ratios increased with

372   residence times (Fig. 5) and decreased with flow rates (Fig. ~~S4~~S7), and a larger flow rate would be

373   preferred if the losses are to be reduced to acceptable levels.

374   Adsorptive losses may vary with VOC species. The loss is generally related to vapor pressure, which

375   is modified by molecular weight and boiling point (Ortega and Helmig, 2008). As a result, heavier

376   VOCs like α-pinene and β-caryophyllene with lower vapor pressure are easier to be adsorbed. Kolari

377   et al. (2012) observed that heavier VOCs (m/z > 100) such as hexanal and MTs showed stronger

378   adsorption in their dynamic chamber. Schaub et al. (2010) also found stronger adsorption for SQTs

379 in a branch chamber where weaker adsorption occurred at higher temperature. Our results also

380 demonstrated that running conditions like flow rates are needed to be carefully modulated especially

381 for heavier BVOCs like MTs and SQTs.

3.2.2 Influence of RH on Transfer efficiency

383 The influence of RH on transfer efficiencies or adsorptive loss of BVOC in a chamber is not so

384 consistent in previous studies. While Kolari et al. (2012) observed notable adsorptive loss for

385 isoprene and methyl vinyl ketone at wet environment and no significant differences between wet

386 and dry environment for hexanal and α-pinene, Hohaus et al. (2016) observed transfer efficiencies

387 independent on RH (ranging 25-100 %) for VOCs with different vapor pressure and polarity through

388 the "PLant chamber Unit for Simulation (PLUS)". In this study, transfer efficiency under different

389 RH (0 %, 20 %, 40 %, 60 %, 80 %, 100 %) and flow rates (3, 6, 9, 12, 15 L min^{-1}) were further

390 investigated with the standard VOCs mixture (Fig. 2).

391 As showed in Fig. 6, unlike flow rates, RH seemed to have less influence on transfer efficiencies,

392 as reflected by the relative standard deviation (RSD) of transfer efficiencies at different RH. The

393 RSD of transfer efficiencies under different RH varied from 2.6 % for acetone at 15 L min^{-1} to 14.8 %

394 for sesquiterpene at 3 L min^{-1}. There is no consistent decreasing or increasing trend for transfer

395 efficiencies with the increase of RH. Instead, the influence of RH on transfer efficiencies showed

396 compound specific patterns. For acetonitrile and methylacrolein, the highest transfer efficiency

397 occurred at low RH=0 % (dry air); for α-pinene and β-caryophyllene, the highest transfer efficiency

398 occurred under higher RH (100 %); for acrylonitrile, acetone and isoprene, higher transfer efficiency

399 occurred at medium humidity levels (~40 %); and for acrolein, transfer efficiencies were close to

400 each other under different RH, agreeing to the results by Hohaus et al. (2016). Theoretically, the

401 influence of RH on adsorptive loss depends on the competition of adsorption sites by water

402 molecules on the surfaces and the modification of energy spectrum of the adsorption sites by

403 condensed water on the surfaces. Therefore, for water-insoluble or hydrophobic BVOCs like

404 isoprene, MTs and SQTs, higher RH may help suppress their uptake on surfaces, while for water

405 soluble or hydrophilic OVOCs, lower RH would be preferred for higher transfer efficiencies.

3.2.3 Possible correction of VOCs losses in lab simulations

407 Due to the adsorptive losses, the measured emission rates from plant leaves would be

408 underestimated, particularly for those with unsatisfactory transfer efficiencies even under high flow

409 rates and short residence times. If the adsorptive loss rate is simplified to be linearly proportional to

410 the VOC concentration inside the chamber, Eq. (1) can be rewritten as:

411
$$V \frac{dC}{dt} = E - F \times (C - C_0) - k \times C \qquad (6)$$

412 where k is the correction factor due to adsorptive loss. When the VOC concentration in the chamber

413 reaches steady state C_s, the emission rates can be estimated as:

414
$$E = F \times (C_s - C_0) + k \times C_s \qquad (7)$$

415 In our simulation tests in the lab with the standard mixtures with the known E and F, after measuring

416 the steady state concentration C_s, based on above Eq. (6) we could calculate the adsorptive loss term

417 $k \times C_s$ and k as well.

418 The correction factors for different VOCs at different flow rates and RH are presented in Table S4.

419 Consistent with the lower transfer efficiencies at lower flow rates, for a VOC species, the largest k

420 value occurs at 3 L min^{-1} while the smallest k value occurs at 15 L min^{-1}. Also k is less affected by

421 RH than by flow rates, and varies among the VOCs probably due to their different adsorptive

422 behavior on the surfaces.

423 It is under question, however, if this kind of simplified loss correction in lab simulations can be

424 applicable to field measurements due to complex adsorption behavior. For example, in field

425 measurements of branch-scale emissions, the surfaces may have limited adsorption capacity

426 especially for the Teflon-coated inner walls, and thus with the prolonged enclosure time of a branch

427 in the chamber, some species may become adsorption saturated on the surfaces and thus would be

428 less affected by the adsorptive loss. To avoid the influence of VOCs adsorption, it may be a plausible

429 way to measure emissions after getting adsorption saturation (Chen et al., 2019). In the field, one to

430 two hours of balance time prior to tests will be set to reduce the artificial disturbance to the

431 physiological state of the enclosed branch and to ensure that emissions in the enclosure get stabilized,

432 such procedure would also set enough time for adsorption of emitted compounds and thereby benefit

433 lowering the adsorptive loss during tests afterwards. On the other hand, adsorption of VOCs on

434 surfaces in the enclosure will be weakened at high temperatures (Schaub et al., 2010; Kolari et al.,

435 2012). Some more adsorptive species, like SQTs, after getting adsorption saturated at lower

436 temperature, would release again from the surface when air temperature elevated (Schaub et al.,

437 2010). Consider the temperature effect on the adsorptive loss, field enclosure measurements of

438 branch-scale emissions at higher temperature intervals (e.g. near noon time) during a day would

439 have less interferences by adsorptive loss.

440 Despite of the limitation of loss correction from the lab simulation in this study, this approach might

441 be implicative to deal with the more complex adsorption behavior in field measurements. Previous

442 lab studies also eliminated loss by using VOCs standards to calibrate the whole measuring system

443 (Ghirardo et al., 2011; 2020). Ortega et al. (2008) made adsorption loss corrections of VOCs by

444 adding internal standard into the enclosure to calculate the recovery. Therefore, for more accurate

445 emission measurements by dynamic enclosures in the field, adding surrogate compounds in the

446 circulating air in the same way as this simulation study (Fig. 2) would be a possible way to evaluate

447 *in situ* transfer efficiencies.

448 **3.3 Comparison of environmental parameters inside and outside of the chamber in field**

449 **measurements**

450 When conducting field measurements of BVOCs with branch enclosures, it is vital that

451 environmental parameters, particularly temperature, resemble the natural growing conditions and

452 are not seriously deviated due to enclosure. As temperature will affect the emission of BVOCs from

453 plants in an exponential way mainly due to the fact that temperature can modify the activity of

454 biosynthetic enzymes, the vapor pressures and the cellular diffusion rates of BVOCs

455 (Laothawornkitkul et al., 2009), and a small change in leaf temperature may induce big variation in

456 BVOCs emissions. Here we first conducted tests about the influence of flow rates (3-15 L min^{-1}) on

457 the differences in temperature and RH between ambient and enclosure, then we conducted tests for

458 *Pinus massoniana* at a medium flow rate of 9 L min^{-1}.

459 **3.3.1 Enclosure-ambient T/RH differences under different flow rates**

460 As showed in Fig. 7, when conducting tests of BVOCs emissions (Fig. S5S8) with a branch of

461 *Mangifera indica* (~7 g dry mass of leaves) under ambient air temperature of 31-33 °C and PAR of

462 1000-1200 μmol m^{-2} s^{-1}, the differences in both temperature and RH between enclosure and ambient

463 air decreased sharply with the increase of flow rates. As flow rates increased from 3 L min^{-1}

464 (residence time ~4.5 min) to 15 L min^{-1} (residence time ~0.9 min), the enclosure-ambient

465 temperature differences (ΔT) decreased from 4.5±0.3 to 1.0±0.2 °C (Fig. 7a), the RH differences

466 (ΔRH) decreased from 9.8±0.5 % to 1.2±0.1 % (Fig. 7b). The results confirmed that the ambient-

467 enclosure differences in T/RH could be largely reduced if enclosure air is sufficiently circulated. It

468 seemed that at a flow rate of 9 L min^{-1} (residence time ~1.5 min), the differences could be fairly

469 satisfactory (ΔT < 2°C; ΔRH < 5 %).

3.3.2 Enclosure-ambient differences of environmental parameters during field tests of BVOC emissions from *Pinus massoniana*

472 As mentioned above, higher flow rates will result in lower steady state concentrations. To guarantee

473 the detection of BVOCs species (Fig. S8) with very low emission rates, we only adopted a medium

474 flow rate of 9 L min^{-1} when conducting tests on a pine (*Pinus massoniana*) tree to compare the

475 environmental parameters inside and outside the enclosure. As mentioned above, higher flow rates

476 will result in lower steady state concentrations. To guarantee the detection of BVOCs species (Fig.

477 S5) with very low emission rates, we only adopted a medium flow rate of 9 L min^{-1} when conducting

478 tests during 9:00-17:30 on 8 October 2019 with healthy nature-grown branches of a pine (*Pinus*

479 *massoniana*) tree (~20-year-old and ~12 m high) to compare the environmental parameters inside

480 and outside the enclosure.

481

482 As expected, higher temperature and RH but lower PAR and CO_2 concentrations were observed

483 inside than outside the enclosure (Fig. S6S9). On average the temperature deviation inside the

484 chamber was +1.2±1.1 °C, and the RH deviation was +12.8±4.0 %; The CO_2 concentrations inside

485 showed -53 ppm deviation on average with the relative deviation of -(4-15) % during the day. The

486 light transmittance was 92.4±5.4 % on average.

487 Higher temperature inside the chamber could be attributed to the greenhouse effect (Ortega et al.,

488 2008). The temperature deviation inside the chamber in this study is smaller when compared to

489 those reported previously (Fig. 8). The largest relative temperature deviation of 11.4 % was much

490 lower than that of over 50 % reported in previous studies (Fig. 8a). Even under full sunlight at noon

491 a temperature deviation of 4 °C was observed in this study, lower than that of 6-7 °C observed by

492 Helmig et al. (2006), 8 °C by Ortega et al. (2008), and comparable to 3-4 °C by Kolari et al. (2012)

493 (Fig. 8b). Higher RH inside the chamber is caused by leaf transpiration and the +12.8 % deviation

494 is acceptable in field tests. Photosynthetic adsorption by leaves will lead to depletion of CO_2 in the

495 chamber. Kesselmeier et al. (1996) also observed 50 ppm lower CO_2 concentration (relative

496 deviation of -13.2 %) in their chamber due to the depletion, and they considered that it was well

497 within an acceptable range for normal physiological conditions. The light transmittance of 92.4±5.4 %

498 in this study is comparable with those reported in previous studies, such as that of 90 % by Aydin et
499 al. (2014), 92 % by Karlik et al. (2001), 95 % by Chen et al. (2020) and 97 % by Lüpke et al. (2017).
500 The comparison suggests the environmental parameters in the semi-open dynamic chamber were
501 less disturbed. Moreover, tests in this study were conducted at flow rates of 9 L min^{-1} with residence
502 time of 1.5 min, and observed steady state concentrations for major emitted BVOC species (such as
503 ~15 μg m^{-3} for α-pinene) were orders of magnitude higher above their MDLs. Therefore, as
504 discussed above, if we raised flow rates to be as high as 50 min L^{-1} with residence time of ~15
505 seconds, we could still successfully measure the emission rates for the major species, and the
506 equilibrium time, the adsorptive loss, as well as the inside-outside differences of temperature and
507 RH, would be further reduced to a larger extent.

4 Conclusions

509 In order to obtain accurate emission rates of BVOCs from plants growing under natural
510 environment, it is vital for branch-scale enclosure to reduce the adsorptive loss and minimize the
511 disturbance to the natural growing microenvironments. In this study, based on tests in the lab and in
512 the field with a self-made dynamic enclosure, we demonstrated that operational parameters like air
513 circulating rates could impact heavily on the performance of dynamic enclosures, and therefore
514 should be optimized before field applications. As revealed by the results, higher circulating rates
515 could not only reduce the equilibrium time and facilitate higher time resolution emission
516 measurements, but also reduce the adsorptive losses and the enclosure-ambient temperature/RH
517 differences and thus obtain more accurate emission rates under natural conditions. Therefore, in
518 field measurements using the dynamic enclosure method, if advanced analytical techniques like
519 PTR-ToF-MS can assure sensitive enough detections, higher air circulating flow rates are preferred.
520 It is worth noting that although the inner surfaces were coated with inert Teflon films, based on lab
521 simulation with standard mixtures, BVOC species like monoterpenes and sesquiterpenes showed
522 transfer efficiencies less than 70% even the residence times were kept as low as <1 min. This
523 suggests that emission factors of these species from dynamic enclosures might be underestimated if
524 the adsorptive losses were not seriously considered and reduced, and further efforts are needed to
525 develop a certified protocol to assure accurate emission measurements particularly for species (e.g.,
526 monoterpenes and sesquiterpenes) with lower transfer efficiencies.
527 In the future, surrogate compounds like deuterated monoterpenes and sesquiterpenes can be added

528 in the circulating air as did in our lab simulation study, to track the chamber performance and to
529 correct the losses. Ghirardo et al. (2011, 2020) performed calibrations by passing a mixture of VOCs
530 in N_2 through the whole gas exchange system. Inspired by this approach, in field tests deuterated
531 monoterpenes and sesquiterpenes can be doped into circulating air, or deuterated monoterpenes and
532 sesquiterpenes standard mixture can be released into the chamber at a constant flow rate. This way
533 we may both calibrate target species and evaluate chamber performance.

534

535

536 **Author contributions**

537 JQZ designed and characterized the chamber with the support of HNZ, XMW, YLZ and WS. JQZ
538 and HNZ carried out the chamber assessments. JQZ, HNZ and ZFW carried out the BVOCs
539 measurements in the field. JQZ prepared the manuscript with input from all co-authors. XMW and
540 YLZ revised the manuscript.

541

542 **Data availability**

543 Data are available from Zenodo (https://zenodo.org/record/5347841#.YS5YYRQzapo) or request
544 by contacting the corresponding authors (zhang_yl86@gig.ac.cn; wangxm@gig.ac.cn).

545

546 **Supplement**

547 The supplement related to this article is available online.

548

549 **Competing interests**

550 The authors declare that they have no conflict of interests.

551

558

References

Atkinson, R., and Arey, J.: Gas-phase tropospheric chemistry of biogenic volatile organic compounds: a review, Atmos. Environ., 37, S197-S219, https://doi:org/10.1016/S1352-2310(03)00391-1, 2003.

Aydin, Y. M., Yaman, B., Koca, H., Dasdemir, O., Kara, M., Altiok, H., Dumanoglu, Y., Bayram, A., Tolunay, D., Odabasi, M., and Elbir, T.: Biogenic volatile organic compound (BVOC) emissions from forested areas in Turkey: Determination of specific emission rates for thirty-one tree species, Sci. Total Environ., 490, 239-253, https://doi.org/0.1016/j.scitotenv.2014.04.132, 2014.

Bai, J., Guenther, A., Turnipseed, A., Duhl, T., and Greenberg, J.: Seasonal and interannual variations in whole-ecosystem BVOC emissions from a subtropical plantation in China, Atmos. Environ., 161, 176-190, https://doi.org/10.1016/j.atmosenv.2017.05.002, 2017.

Bourtsoukidis, E., Bonn, B., Dittmann, A., Hakola, H., Hellén, H., and Jacobi, S.: Ozone stress as a driving force of sesquiterpene emissions: a suggested parameterisation, Biogeosciences, 9, 4337-4352, 10.5194/bg-9-4337-2012, 2012.

Bourtsoukidis, E., Williams, J., Kesselmeier, J., Jacobi, S., and Bonn, B.: From emissions to ambient mixing ratios: online seasonal field measurements of volatile organic compounds over a Norway spruce-dominated forest in central Germany, Atmos. Chem. Phys., 14, 6495-6510, https://doi.org/10.5194/acp-14-6495-2014, 2014.

Cao, X. L., Boissard, C., Juan, A. J., Hewitt, C. N., and Gallagher, M.: Biogenic emissions of volatile organic compounds from gorse (*Ulex europaeus*): Diurnal emission fluxes at Kelling Heath, England, J. Geophys. Res. Atmos.J. Geophys. Res. Atmos., 102, 18903-18915, https://doi.org/10.1029/97jd00421, 1997.

Chen, J., Bi, H., Yu, X., Fu, Y., and Liao, W.: Influence of physiological and environmental factors on the diurnal variation in emissions of biogenic volatile compounds from *Pinus tabuliformis*, J. Environ. Sci. (China), 81, 102-118, https://doi.org/10.1016/j.jes.2019.01.020, 2019.

Chen, J., Tang, J., and Yu, X.: Environmental and physiological controls on diurnal and seasonal patterns of biogenic volatile organic compound emissions from five dominant woody species under field conditions, Environ. Pollut., 259, 113955, https://doi.org/10.1016/j.envpol.2020.113955, 2020.

Ciccioli, P., Brancaleoni, E., Frattoni, M., Di Palo, V., Valentini, R., Tirone, G., Seufert, G., Bertin, N., Hansen, U., Csiky, O., Lenz, R., and Sharma, M.: Emission of reactive terpene compounds from orange orchards and their removal by within-canopy processes, J. Geophys. Res. Atmos.J. Geophys. Res. Atmos., 104, 8077-8094, https://doi.org/10.1029/1998jd100026, 1999.

Copolovici, L., and Niinemets, Ü.: Flooding induced emissions of volatile signalling compounds in three tree species with differing waterlogging tolerance, Plant, Cell Environ., 33, 1582–1594, https://doi.org/10.1111/j.1365-3040.2010.02166.x, 2010.

de Souza, V. F., Niinemets, U., Rasulov, B., Vickers, C. E., Duvoisin Junior, S., Araujo, W. L., and Goncalves, J. F. C.: Alternative carbon sources for isoprene emission, Trends Plant Sci., 23, 1081-1101, https://doi.org/10.1016/j.tplants.2018.09.012, 2018.

Di Carlo, P., Brune, W. H., Martinez, M., Harder, H., Lesher, R., Ren, X. R., Thornberry, T., Carroll, M. A., Young, V., Shepson, P. B., Riemer, D., Apel, E., and Campbell, C.: Missing OH reactivity in a forest: Evidence for unknown reactive biogenic VOCs, Science, 304, 722-725, https://doi.org/10.1126/science.1094392, 2004.

Douma, J. C., Ganzeveld, L. N., Unsicker, S. B., Boeckler, G. A., and Dicke, M.: What makes a volatile organic compound a reliable indicator of insect herbivory? Plant, Cell Environ., 42, 3308-3325, https://doi.org/10.1111/pce.13624, 2019.

Fang, H., Luo, S., Huang, X., Fu, X., Xiao, S., Zeng, J., Wang, J., Zhang, Y., and Wang, X.: Ambient naphthalene and methylnaphthalenes observed at an urban site in the Pearl River Delta region: Sources and contributions to secondary organic aerosol, Atmos. Environ., 252, https://doi.org/10.1016/j.atmosenv.2021.118295, 2021.

Feng, Z., Yuan, X., Fares, S., Loreto, F., Li, P., Hoshika, Y., and Paoletti, E.: Isoprene is more affected by climate drivers than monoterpenes: A meta-analytic review on plant isoprenoid emissions, Plant, Cell Environ., 42, 1939-1949, https://doi.org/10.1111/pce.13535, 2019.

Ghirardo, A., Gutknecht, J., Zimmer, I., Brueggemann, N., and Schnitzler, J.-P.: Biogenic volatile organic compound and respiratory CO_2 emissions after ^{13}C-Labeling: Online tracing of C translocation dynamics in poplar plants, Plos One, 6, 10.1371/journal.pone.0017393, 2011.

Ghirardo, A., Lindstein, F., Koch, K., Buegger, F., Schloter, M., Albert, A., Michelsen, A., Winkler, J. B., Schnitzler, J. P., and Rinnan, R.: Origin of volatile organic compound emissions from

subarctic tundra under global warming, Glob Chang Biol, 26, 1908-1925, 10.1111/gcb.14935, 2020.

Gonzaga Gomez, L., Loubet, B., Lafouge, F., Ciuraru, R., Buysse, P., Durand, B., Gueudet, J.-C., Fanucci, O., Fortineau, A., Zurfluh, O., Decuq, C., Kammer, J., Duprix, P., Bsaibes, S., Truong, F., Gros, V., and Boissard, C.: Comparative study of biogenic volatile organic compounds fluxes by wheat, maize and rapeseed with dynamic chambers over a short period in northern France, Atmos. Environ., 214, https://doi.org/10.1016/j.atmosenv.2019.116855, 2019.

Gu, D., Guenther, A. B., Shilling, J. E., Yu, H., Huang, M., Zhao, C., Yang, Q., Martin, S. T., Artaxo, P., Kim, S., Seco, R., Stavrakou, T., Longo, K. M., Tota, J., Ferreira de Souza, R. A., Vega, O., Liu, Y., Shrivastava, M., Alves, E. G., Santos, F. C., Leng, G., and Hu, Z.: Airborne observations reveal elevational gradient in tropical forest isoprene emissions, Nat. Commun., 8, 10.1038/ncomms15541, 2017.

Gu, H., Wang, J., Ma, L., Shang, Z., and Zhang, Q.: Insights into the BRT (Boosted Regression Trees) method in the study of the climate-growth relationship of Masson pine in subtropical China, Forests, 10, https://doi.org/10.3390/f10030228, 2019.

Guenther, A., Hewitt, C. N., Erickson, D., Fall, R., Geron, C., Graedel, T., Harley, P., Klinger, L., Lerdau, M., McKay, W. A., Pierce, T., Scholes, B., Steinbrecher, R., Tallamraju, R., Taylor, J., and Zimmerman, P.: A global model of natural volatile organic compound emissions, J. Geophys. Res. -Atmos., 100, 8873-8892, https://doi.org/10.1029/94jd02950, 1995.

Guenther, A., Karl, T., Harley, P., Wiedinmyer, C., Palmer, P. I., and Geron, C.: Estimates of global terrestrial isoprene emissions using MEGAN (Model of Emissions of Gases and Aerosols from Nature), Atmos. Chem. Phys., 6, 3181-3210, https://doi.org/10.5194/acp-6-3181-2006, 2006.

Guenther, A., Jiang, X., Heald, C. L., Sakulyanontvittaya, T., Duhl, T., Emmons, L. K., and Wang, X.: The Model of Emissions of Gases and Aerosols from Nature version 2.1 (MEGAN2.1): an extended and updated framework for modeling biogenic emissions, Geosci. Model Dev., 5, 1471-1492, https://doi.org/10.5194/gmd-5-1471-2012, 2012.

Helin, A., Hakola, H., and Hellén, H.: Optimisation of a thermal desorption-gas chromatography-mass spectrometry method for the analysis of monoterpenes, sesquiterpenes and diterpenes, Atmos. Meas. Tech., 13, 3543-3560, https://doi.org/10.5194/amt-13-3543-2020, 2020.

647 Helmig, D., Bocquet, F., Pollmann, J., and Revermann, T.: Analytical techniques for sesquiterpene
648　　　emission rate studies in vegetation enclosure experiments, Atmos. Environ., 38, 557-572,
649　　　https://doi.org/10.1016/j.atmosenv.2003.10.012, 2004.

650 Helmig, D., Ortega, J., Guenther, A., Herrick, J. D., and Geron, C.: Sesquiterpene emissions from
651　　　loblolly pine and their potential contribution to biogenic aerosol formation in the Southeastern
652　　　US, Atmos. Environ., 40, 4150-4157, https://doi.org/10.1016/j.atmosenv.2006.02.035, 2006.

653 Helmig, D., Ortega, J., Duhl, T., Tanner, D., Guenther, A., Harley, P., Wiedinmyer, C., Milford, J.,
654　　　and Sakulyanontvittaya, T.: Sesquiterpene emissions from pine trees - Identifications, emission
655　　　rates and flux estimates for the contiguous United States, Environ. Sci. Technol., 41,
656　　　https://doi.org/1545-1553, 10.1021/es0618907, 2007.

657 Helmig, D., Daly, R. W., Milford, J., and Guenther, A.: Seasonal trends of biogenic terpene
658　　　emissions, Chemosphere, 93, 35-46, https://doi.org/10.1016/j.chemosphere.2013.04.058, 2013.

659 Hohaus, T., Kuhn, U., Andres, S., Kaminski, M., Rohrer, F., Tillmann, R., Wahner, A., Wegener, R.,
660　　　Yu, Z., and Kiendler-Scharr, A.: A new plant chamber facility, PLUS, coupled to the
661　　　atmosphere simulation chamber SAPHIR, Atmos. Meas. Tech., 9, 1247-1259,
662　　　https://doi.org/10.5194/amt-9-1247-2016, 2016.

663 Holopainen, J. K., Kivimäenpää, M., and Nizkorodov, S. A.: Plant-derived secondary organic
664　　　material in the air and ecosystems, Trends Plant Sci., 22, 744-753,
665　　　https://doi.org/10.1016/j.tplants.2017.07.004, 2017.

666 Huang, X., Lai, J., Liu, Y., Zheng, L., Fang, X., Song, W., and Yi, Z.: Biogenic volatile organic
667　　　compound emissions from *Pinus massoniana* and *Schima superba* seedlings: Their responses
668　　　to foliar and soil application of nitrogen, Sci. Total Environ., 705, 135761,
669　　　https://doi.org/10.1016/j.scitotenv.2019.135761, 2020.

670 Huang, Z., Zhang, Y., Yan, Q., Zhang, Z., and Wang, X.: Real-time monitoring of respiratory
671　　　absorption factors of volatile organic compounds in ambient air by proton transfer reaction
672　　　time-of-flight mass spectrometry, J. Hazard. Mater., 320, 547-555,
673　　　https://doi.org/10.1016/j.jhazmat.2016.08.064, 2016.

674 Jing, X., Lun, X., Fan, C., and Ma, W.: Emission patterns of biogenic volatile organic compounds
675　　　from dominant forest species in Beijing, China, J. Environ. Sci. (China), 95, 73-81,
676　　　https://doi.org/10.1016/j.jes.2020.03.049, 2020.

677   Kajos, M. K., Hakola, H., Holst, T., Nieminen, T., Tarvainen, V., Maximov, T., Petäjä, T., Arneth,
678   A., and Rinne, J.: Terpenoid emissions from fully grown east Siberian *Larix cajanderi* trees,
679   Biogeosciences, 10, 4705-4719, https://doi.org/10.5194/bg-10-4705-2013, 2013.

680   Karlik, J. F., and Winer, A. M.: Measured isoprene emission rates of plants in California landscapes:
681   comparison to estimates from taxonomic relationships, Atmos. Environ., 35, 1123-1131,
682   https://doi.org/10.1016/s1352-2310(00)00258-2, 2001.

683   Kesselmeier, J., Schafer, L., Ciccioli, P., Brancaleoni, E., Cecinato, A., Frattoni, M., Foster, P., Jacob,
684   V., Denis, J., Fugit, J. L., Dutaur, L., and Torres, L.: Emission of monoterpenes and isoprene
685   from a Mediterranean oak species *Quercus ilex* L. measured within the BEMA (Biogenic
686   Emissions in the Mediterranean Area) project, Atmos. Environ., 30, 1841-1850,
687   https://doi.org/10.1016/1352-2310(95)00376-2, 1996.

688   Kim, J. C.: Factors controlling natural VOC emissions in a southeastern US pine forest, Atmos.
689   Environ., 35, 3279-3292, https://doi.org/10.1016/s1352-2310(00)00522-7, 2001.

690   Kleist, E., Mentel, T. F., Andres, S., Bohne, A., Folkers, A., Kiendler-Scharr, A., Rudich, Y., Springer,
691   M., Tillmann, R., and Wildt, J.: Irreversible impacts of heat on the emissions of monoterpenes,
692   sesquiterpenes, phenolic BVOC and green leaf volatiles from several tree species,
693   Biogeosciences, 9, 5111-5123, https://doi.org/10.5194/bg-9-5111-2012, 2012.

694   Kolari, P., Back, J., Taipale, R., Ruuskanen, T. M., Kajos, M. K., Rinne, J., Kulmala, M., and Hari,
695   P.: Evaluation of accuracy in measurements of VOC emissions with dynamic chamber system,
696   Atmos. Environ., 62, 344-351, 10.1016/j.atmosenv.2012.08.054, 2012.

697   Laothawornkitkul, J., Taylor, J. E., Paul, N. D., and Hewitt, C. N.: Biogenic volatile organic
698   compounds in the earth system, New Phytol., 183, 27-51, https://doi.org/10.1111/j.1469-
699   8137.2009.02859.x, 2009.

700   Li, L., Guenther, A. B., Xie, S., Gu, D., Seco, R., Nagalingam, S., and Yan, D.: Evaluation of semi-
701   static enclosure technique for rapid surveys of biogenic volatile organic compounds (BVOCs)
702   emission measurements, Atmos. Environ., 212, 1-5,
703   https://doi.org/10.1016/j.atmosenv.2019.05.029, 2019.

704   Loreto, F., and Schnitzler, J.-P.: Abiotic stresses and induced BVOCs, Trends Plant Sci., 15, 154-
705   166, https://doi.org/10.1016/j.tplants.2009.12.006, 2010.

706 Lüpke, M., Steinbrecher, R., Leuchner, M., and Menzel, A.: The Tree Drought Emission MONitor
707   (Tree DEMON), an innovative system for assessing biogenic volatile organic compounds
708   emission from plants, Plant Methods, 13, 14, 10.1186/s13007-017-0166-6, 2017.

709 Matsunaga, S. N., Mochizuki, T., Ohno, T., Endo, Y., Kusumoto, D., and Tani, A.: Monoterpene and
710   sesquiterpene emissions from Sugi (*Cryptomeria japonica*) based on a branch enclosure
711   measurements, Atmos. Pollut. Res., 2, 16-23, https://doi.org/10.5094/apr.2011.003, 2011.

712 Mermet, K., Sauvage, S., Dusanter, S., Salameh, T., Léonardis, T., Flaud, P.-M., Perraudin, É.,
713   Villenave, É., and Locoge, N.: Optimization of a gas chromatographic unit for measuring
714   biogenic volatile organic compounds in ambient air, Atmos. Meas. Tech., 12, 6153-6171,
715   https://doi.org/10.5194/amt-12-6153-2019, 2019.

716 Mozaffar, A., Schoon, N., Digrado, A., Bachy, A., Delaplace, P., du Jardin, P., Fauconnier, M. L.,
717   Aubinet, M., Heinesch, B., and Amelynck, C.: Methanol emissions from maize: Ontogenetic
718   dependence to varying light conditions and guttation as an additional factor constraining the
719   flux, Atmos. Environ., 152, 405-417, https://doi.org/10.1016/j.atmosenv.2016.12.041, 2017.

720 Niinemets, U., Kuhn, U., Harley, P. C., Staudt, M., Arneth, A., Cescatti, A., Ciccioli, P., Copolovici,
721   L., Geron, C., Guenther, A., Kesselmeier, J., Lerdau, M. T., Monson, R. K., and Penuelas, J.:
722   Estimations of isoprenoid emission capacity from enclosure studies: measurements, data
723   processing, quality and standardized measurement protocols, Biogeosciences, 8, 2209-2246,
724   https://doi.org/10.5194/bg-8-2209-2011, 2011.

725 Ortega, J., and Helmig, D.: Approaches for quantifying reactive and low-volatility biogenic organic
726   compound emissions by vegetation enclosure techniques - part A, Chemosphere, 72, 343-364,
727   https://doi.org/10.1016/j.chemosphere.2007.11.020, 2008.

728 Ortega, J., Helmig, D., Daly, R. W., Tanner, D. M., Guenther, A. B., and Herrick, J. D.: Approaches
729   for quantifying reactive and low-volatility biogenic organic compound emissions by vegetation
730   enclosure techniques - Part B: Applications, Chemosphere, 72, 365-380,
731   https://doi.org/10.1016/j.chemosphere.2008.02.054, 2008.

732 Pape, L., Ammann, C., Nyfeler-Brunner, A., Spirig, C., Hens, K., and Meixner, F. X.: An automated
733   dynamic chamber system for surface exchange measurement of non-reactive and reactive trace
734   gases of grassland ecosystems, Biogeosciences, 6, 405–429, https://doi.org/10.5194/bg-6-405-
735   2009, 2009.

Peñuelas~~Penuelas~~, J., Rutishauser, T., and Filella, I.: Phenology feedbacks on climate change, Science, 324, 887-888, https://doi.org/10.1126/science.1173004, 2009.

Pokorska, O., Dewulf, J., Amelynck, C., Schoon, N., Simpraga, M., Steppe, K., and Van Langenhove, H.: Isoprene and terpenoid emissions from *Abies alba*: Identification and emission rates under ambient conditions, Atmos. Environ., 59, 501-508, https://doi.org/10.1016/j.atmosenv.2012.04.061, 2012.

Pollmann, J., Ortega, J., and Helmig, D.: Analysis of atmospheric sesquiterpenes: Sampling losses and mitigation of ozone interferences, Environ. Sci. Technol., 39, 9620-9629, https://doi.org/10.1021/es050440w, 2005.

Rhoderick, G. C., and Lin, J.: Stability assessment of gas mixtures containing monoterpenes in varying cylinder materials and treatments, Anal. Chem., 85, 4675-4685, https://doi.org/10.1021/ac400324v, 2013.

Rinne, J., Taipale, R., Markkanen, T., Ruuskanen, T. M., Hellen, H., Kajos, M. K., Vesala, T., and Kulmala, M.: Hydrocarbon fluxes above a Scots pine forest canopy: measurements and modeling, Atmos. Chem. Phys., 7, 3361-3372, https://doi.org/10.5194/acp-7-3361-2007, 2007.

Schaub, A., Blande, J. D., Graus, M., Oksanen, E., Holopainen, J. K., and Hansel, A.: Real-time monitoring of herbivore induced volatile emissions in the field. Physiol. Plant., 138, 123–133, https://doi:10.1111/j.1399-3054.2009.01322.x, 2010.

Scott, C. E., Arnold, S. R., Monks, S. A., Asmi, A., Paasonen, P., and Spracklen, D. V.: Substantial large-scale feedbacks between natural aerosols and climate, Nat. Geosci., 11, 44-48, 10.1038/s41561-017-0020-5, 2017.

Šimpraga, M., Takabayashi, J., and Holopainen, J. K.: Language of plants: Where is the word? J. Integr. Plant Biol., 58, 343-349, https://doi.org/10.1111/jipb.12447, 2016.

Simpson, D., Winiwarter, W., Borjesson, G., Cinderby, S., Ferreiro, A., Guenther, A., Hewitt, C. N., Janson, R., Khalil, M. A. K., Owen, S., Pierce, T. E., Puxbaum, H., Shearer, M., Skiba, U., Steinbrecher, R., Tarrason, L., and Oquist, M. G.: Inventorying emissions from nature in Europe, J. Geophys. Res. -Atmos., 104, 8113-8152, https://doi.org/10.1029/98jd02747, 1999.

Situ, S., Wang, X., Guenther, A., Zhang, Y., Wang, X., Huang, M., Fan, Q., and Xiong, Z.: Uncertainties of isoprene emissions in the MEGAN model estimated for a coniferous and

broad-leaved mixed forest in Southern China, Atmos. Environ., 98, 105-110, https://doi.org/10.1016/j.atmosenv.2014.08.023, 2014.

Spirig, C., Neftel, A., Ammann, C., Dommen, J., Grabmer, W., Thielmann, A., Schaub, A., Beauchamp, J., Wisthaler, A., and Hansel, A.: Eddy covariance flux measurements of biogenic VOCs during ECHO 2003 using proton transfer reaction mass spectrometry, Atmos. Chem. Phys., 5, https://doi.org/465-481, 10.5194/acp-5-465-2005, 2005.

van Meeningen, Y., Wang, M., Karlsson, T., Seifert, A., Schurgers, G., Rinnan, R., and Hoist, T.: Isoprenoid emission variation of Norway spruce across a European latitudinal transect, Atmos. Environ., 170, 45-57, https://doi.org/10.1016/j.atmosenv.2017.09.045, 2017.

Wang, G., Guan, D., Xiao, L., and Peart, M. R.: Forest biomass-carbon variation affected by the climatic and topographic factors in Pearl River Delta, South China, J. Environ. Manage., 232, 781-788, https://doi.org/10.1016/j.jenvman.2018.11.130, 2019.

Wang, X., Liu, T., Bernard, F., Ding, X., Wen, S., Zhang, Y., Zhang, Z., He, Q., Lü, S., Chen, J., Saunders, S., and Yu, J.: Design and characterization of a smog chamber for studying gas-phase chemical mechanisms and aerosol formation, Atmos. Meas. Tech., 7, 301-313, https://doi.org/10.5194/amt-7-301-2014, 2014.

Wang, X. M., Situ, S. P., Guenther, A., Chen, F., Wu, Z. Y., Xia, B. C., and Wang, T. J.: Spatiotemporal variability of biogenic terpenoid emissions in Pearl River Delta, China, with high-resolution land-cover and meteorological data, Tellus Ser. B-Chem. Phys. Meteorol., 63, 241-254, https://doi.org/10.1111/j.1600-0889.2010.00523.x, 2011.

Wiß~~Wiss~~, F., Ghirardo, A., Schnitzler, J.-P., Nendel, C., Augustin, J., Hoffmann, M., and Grote, R.: Net ecosystem fluxes and composition of biogenic volatile organic compounds over a maize field-interaction of meteorology and phenological stages, Glob Change Biol Bioenergy, 9, 1627-1643, https://doi.org/10.1111/gcbb.12454, 2017.

Yaman, B., Aydin, Y. M., Koca, H., Dasdemir, O., Kara, M., Altiok, H., Dumanoglu, Y., Bayram, A., Tolunay, D., Odabasi, M., and Elbir, T.: Biogenic Volatile Organic Compound (BVOC) emissions from various endemic tree species in Turkey, Aerosol Air Qual. Res., 15, 341-356, https://doi.org/10.4209/aaqr.2014.04.0082, 2015.

Yáñez-Serrano, A. M., Mahlau, L., Fasbender, L., Byron, J., Williams, J., Kreuzwieser, J., and Werner, C.: Heat stress increases the use of cytosolic pyruvate for isoprene biosynthesis, J. Exp. Bot., 70, 5827-5838, https://doi.org/10.1093/jxb/erz353, 2019.

Zhang, H., Zhang, Y., Huang, Z., Acton, W. J. F., Wang, Z., Nemitz, E., Langford, B., Mullinger, N., Davison, B., Shi, Z., Liu, D., Song, W., Yang, W., Zeng, J., Wu, Z., Fu, P., Zhang, Q., and Wang, X.: Vertical profiles of biogenic volatile organic compounds as observed online at a tower in Beijing, J. Environ. Sci. (China), 95, 33-42, https://doi.org/10.1016/j.jes.2020.03.032, 2020.

Zhang, Y., Zhang, R., Yu, J., Zhang, Z., Yang, W., Zhang, H., Lyu, S., Wang, Y., Dai, W., Wang, Y., and Wang, X.: Isoprene mixing ratios measured at twenty sites in China during 2012–2014: Comparison with model simulation, J. Geophys. Res. Atmos., 125, https://doi.org/10.1029/2020jd033523, 2020.

Figure captions

Figure 1. Photographs and s~~S~~chematic diagram of the semi-open dynamic chamber system for field measurements of BVOCs from plant leaves. (a) and (b) are real photographs of the chamber in the field: (1) T/RH sensors, (2) Teflon fan and electric motor, (3) PAR sensor, (4) Teflon tube for sampling ambient air (C_0), (5) Ozone scrubber, (6) Teflon tube for sampling chamber air, (7) Teflon tube for main airflow, (8) Thermocouples (red circle) for leaf temperature, (9) Thermocouples (red lines) for chamber air temperature. (c) schematic diagram of the chamber system. MFC refers to abbreviation of mass flow controller. LT and AT refer to leaf temperature and air temperature, respectively.

Figure 2. Schematic diagram of chamber characterization experiments in the laboratory using standard BVOCs mixture to imitate emissions of BVOCs from branches. MFC: mass flow controller.

Figure 3. Changes of BVOCs concentrations in the chamber during lab simulation experiments. The black dashed lines are background concentrations. Blue solid lines represent the theoretically predicted BVOCs concentrations in the chamber. The green circles are concentrations measured by the PTR-ToF-MS. Green solid lines represent fitted BVOCs concentrations in the chamber.

Figure 4. Transfer efficiencies of BVOCs when passing through the chamber under different flow rates in the lab simulation experiments. Error bars represents standard deviations of triplicate measurements.

Figure 5. Changes of BVOCs loss ratios (mean ± 1σ, n=5) with residence times.

Figure 6. Influence of relative humidity and flow rates on transfer efficiencies of BVOCs: (a) acetonitrile; (b) acrylonitrile; (c) acrolein; (d) acetone; (e) isoprene; (f) methylacrolein; (g) α-pinene; and (h) β-caryophyllene.~~, (a)-(h) represents acetonitrile, acrylonitrile, acrolein, acetone, isoprene, methylacrolein, α-pinene and β-caryophyllene, respectively.~~

Figure 7. Enclosure-ambient differences in temperature (a) and RH (b) under different flow rates. Circles with errors bars are the measured means and standard deviations. The solid lines are exponential fit curves~~fitted changes~~.

Figure 8. Comparison of temperature deviation (°C) and relative temperature deviation (%) with that reported in previous studies: (a) temperature deviation versus ambient temperature, error bars represent 1σ of deviation; (b) temperature deviation (°C) under normal and full sunlight ~~in~~ for different enclosures. Bars are ranges of temperature deviation while points indicate average
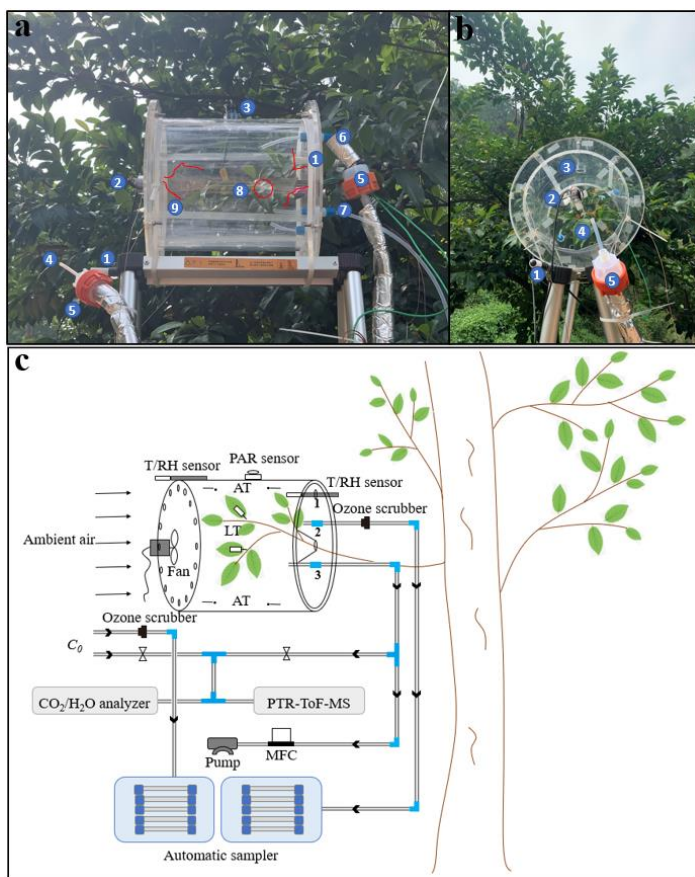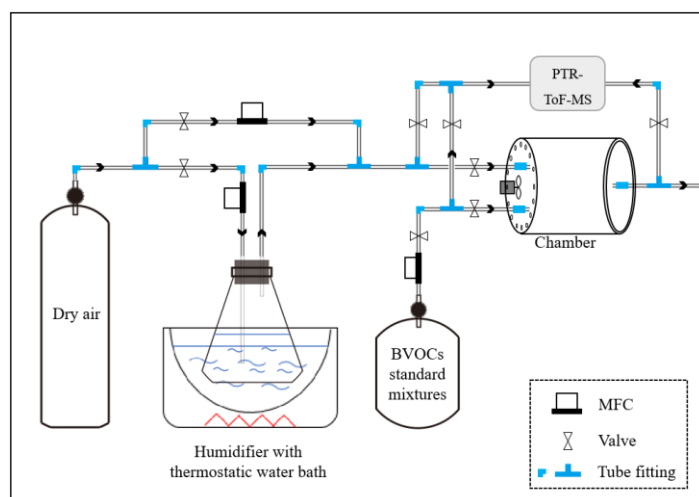
834   temperature deviation.

835

836

34

837

Figure 1. Photographs and sSchematic diagram of the semi-open dynamic chamber system for field measurements of BVOCs from plant leaves. (a) and (b) are real photographs of the chamber in the field: (1) T/RH sensors, (2) Teflon fan and electric motor, (3) PAR sensor, (4) Teflon tube for sampling ambient air (C_0), (5) Ozone scrubber, (6) Teflon tube for sampling chamber air, (7) Teflon tube for main airflow, (8) Thermocouples (red circle) for leaf temperature, (9) Thermocouples (red lines) for chamber air temperature. (c) schematic diagram of the chamber system. MFC refers to abbreviation of mass flow controller. LT and AT refer to leaf temperature and air temperature, respectively.

846

847
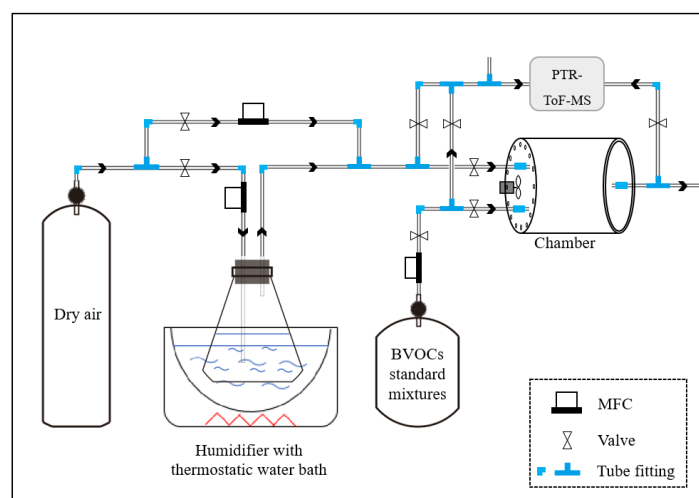
848

Figure 2. Schematic diagram of chamber characterization experiments in the laboratory using standard BVOCs mixture to imitate emissions of BVOCs from branches. MFC: mass flow controller.

851
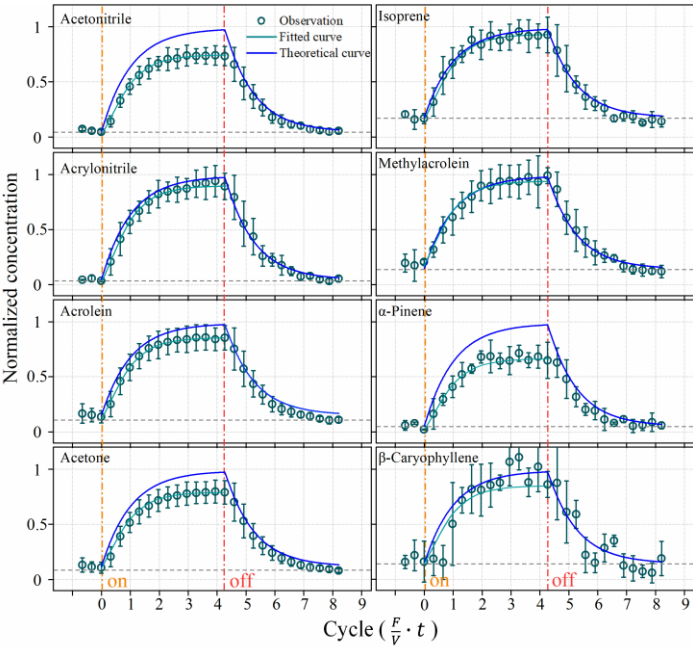
852

Figure 3. Changes of BVOCs concentrations in the chamber during lab simulation experiments. The black dashed lines are background concentrations. Blue solid lines represent the theoretically predicted BVOCs concentrations in the chamber. The green circles are concentrations measured by the PTR-ToF-MS. Green solid lines represent fitted BVOCs concentrations in the chamber.

857
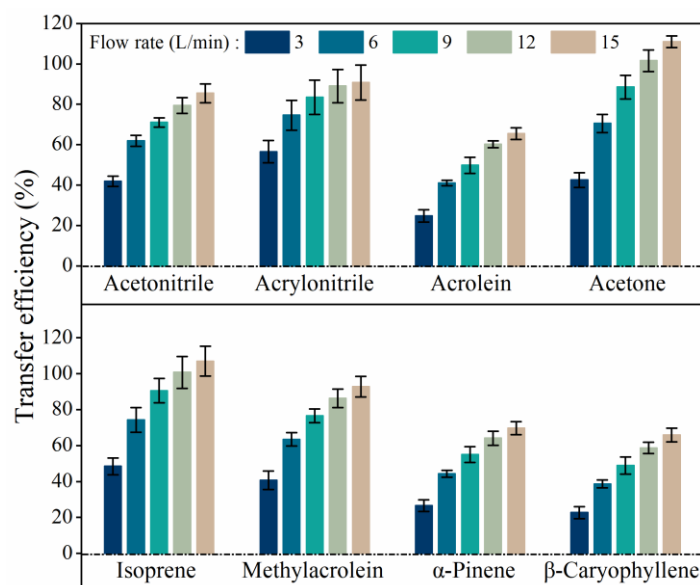
858

859   Figure 4. Transfer efficiencies of BVOCs when passing through the chamber under different flow

860   rates in the lab simulation experiments. Error bars represents standard deviations of triplicate
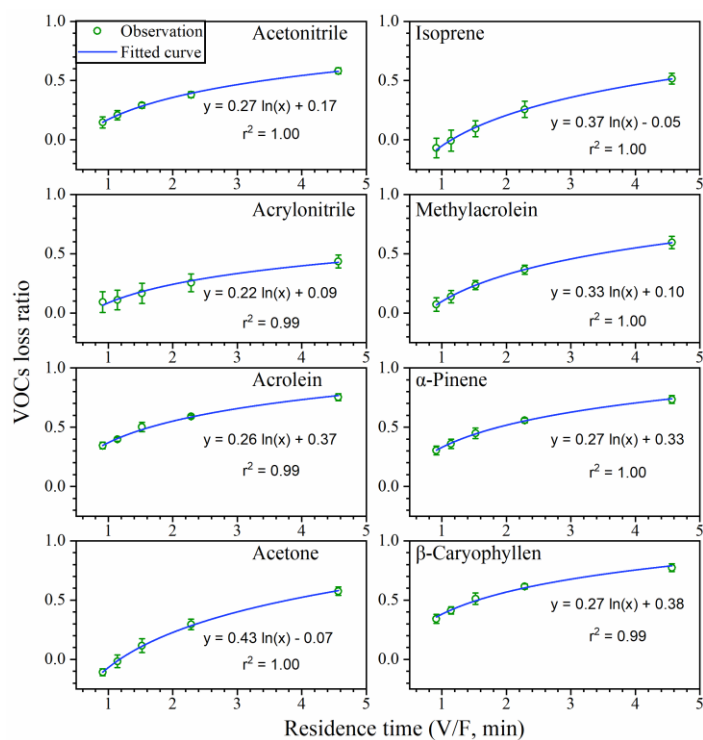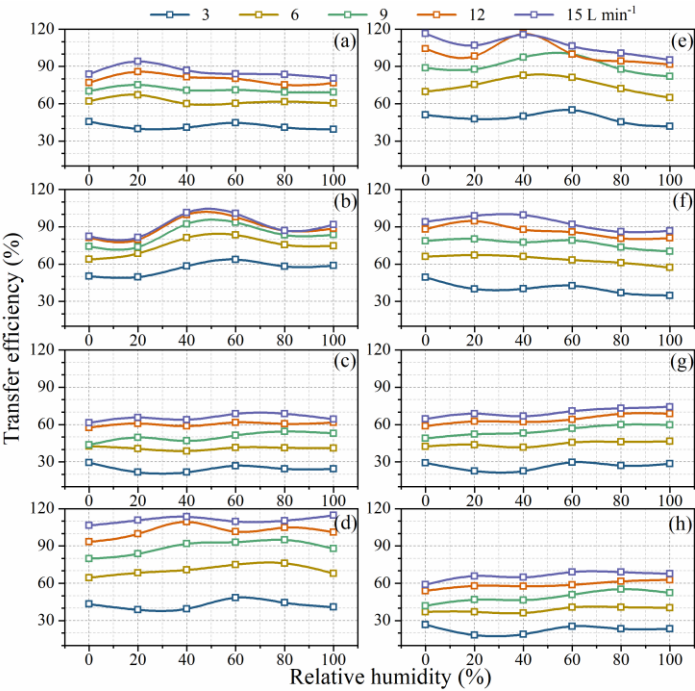
861   measurements.

862

Figure 5. Changes of BVOCs loss ratios (mean ± 1σ, n=5) with residence times.

864
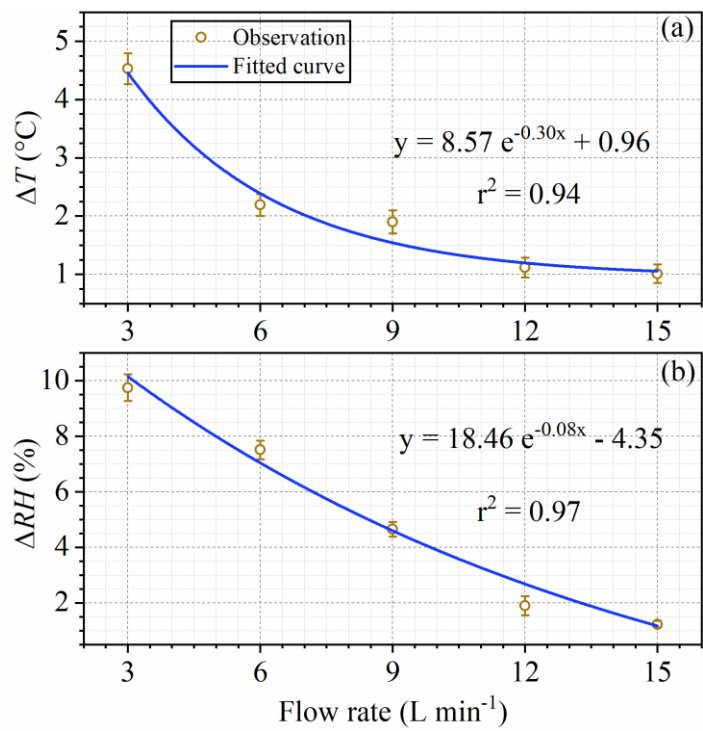
865

866

Figure 6. Influence of relative humidity and flow rates on transfer efficiencies of BVOCs; (a) (h) represents (a) acetonitrile; (b) acrylonitrile; (c) acrolein; (d) acetone; (e) isoprene; (f) methylacrolein; (g) α-pinene; and (h) β-caryophyllene, respectively.

870

871

(a)

$y = 8.57\ e^{-0.30x} + 0.96$

$r^2 = 0.94$

(b)

$y = 18.46\ e^{-0.08x} - 4.35$

$r^2 = 0.97$

872

873   Figure 7. Enclosure-ambient differences in temperature (a) and RH (b) under different flow rates.

874   Circles with errors bars are the measured means and standard deviations. The solid lines are ~~fitted~~

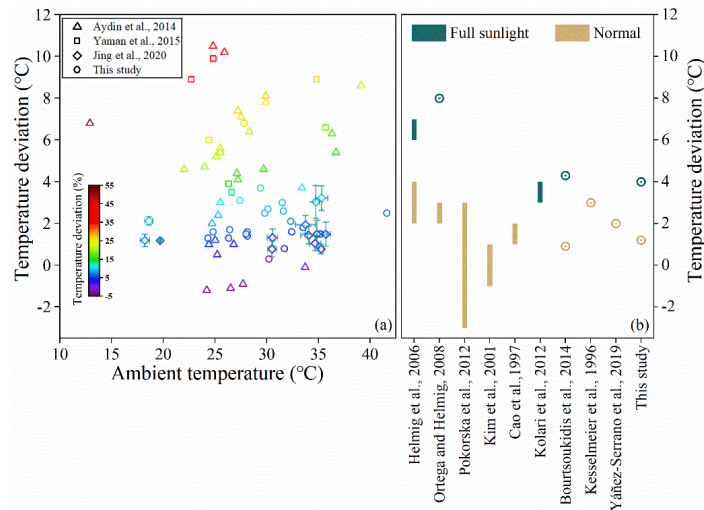875   ~~changes~~exponential fit curves.

876

877

Figure 8. Comparison of temperature deviation (°C) and relative temperature deviation (%) with
that reported in previous studies: (a) temperature deviation versus ambient temperature, error bars
represent 1σ of deviation; (b) temperature deviation (°C) under normal and full sunlight in for
different enclosures. Bars are ranges of temperature deviation while points indicate average
temperature deviation.